

HTL quasiparticle models of deconfined QCD at finite chemical potential

A. Rebhan and P. Romatschke

Institut für Theoretische Physik, Technische Universität Wien, A-1040 Vienna, Austria

Using quasiparticle models and imposing thermodynamic consistency, lattice data for the equation of state of deconfined QCD can be mapped to finite chemical potential. We consider a refinement of existing simple massive quasiparticle models using the non-local hard-thermal-loop (HTL) propagators, and certain NLO corrections thereof, to obtain the thermodynamic potential as a function of temperature and chemical potential. At small chemical potential we find that the results for the slope of constant pressure from our main model for 2 massless quark flavors is in good agreement with recent lattice data for 2+1 flavors while it deviates somewhat from lattice data for 2 flavors from another group. For zero temperature, we obtain an estimate for the critical chemical potential which is close to that obtained from simpler quasiparticle models.

I. INTRODUCTION

Asymptotic freedom suggests that at sufficiently high temperature and/or quark chemical potential QCD is deconfined, i.e. can be described in terms of the fundamental quark and gluonic degrees of freedom [1]. High temperature and small chemical potential are of relevance to the quest for the quark-gluon plasma in heavy-ion experiments; sufficiently high chemical potential (at comparatively low temperature) may be reached in the cores of compact stars. In the latter case, novel color superconducting phases may occur [2], which should however have only comparatively small effects on the equation of state.

The thermodynamic pressure of QCD at high temperature $T \ll \Lambda_{\text{QCD}}$ has been determined in perturbation theory to order $\alpha_s^{5/2}$ in QCD [3, 4] and even to $\alpha^3 \log \alpha$ in a recent heroic effort [5]. Strict perturbation theory, however, shows extremely poor convergence for any temperature of practical interest so that further resummations appear to be necessary. In recent years, resummations which are based on the hard-thermal-loop (HTL) effective action [6] have been proposed, alternatively in form of so-called HTL perturbation theory [7, 8] or based upon the 2-loop Φ -derivable approximation [9, 10, 11] (see also Peshier [12]). The latter approach, which assumes weakly interacting quasiparticles as determined by the HTL propagators and NLO corrections thereof, leads to results which agree remarkably well with lattice data down to about $3T_c$ if standard 2-loop running α_s is adopted,¹ and it has been recently shown that these results are in fact consistent with those obtained in high-order perturbation theory if the latter is organized through effective (dimensionally reduced) field theory according to [14] and effective-field-theory parameters are kept without further expanding in powers of the coupling [13], as already advocated in Ref. [5].

The behavior of the thermodynamic potentials closer to the transition temperature needs to be studied by fully non-perturbative means. For zero quark chemical potential $\mu = 0$ lattice QCD calculations are seemingly up to the task of determining thermodynamic quantities for a quark-gluon plasma very accurately by now [15, 16]. Although recently there has been important progress also for non-vanishing μ [17, 18, 19, 20, 21, 22], the case of large $\mu \gg T$ (relevant for the equation of state for cold dense matter, which is of importance in astrophysical situations [23, 24, 25, 26]) is

¹ This is in fact not the case for 2-loop HTL perturbation theory [8], but it appears that the source of the difficulty has to do with the necessity of thermal counter-terms and incompletely compensated hard contributions, see Ref. [13].

currently beyond the reach of lattice calculations.

As a remedy for this situation, Peshier *et al.* [23, 24] proposed a method which can be used to map the available lattice data for $\mu = 0$ to finite μ and small temperatures by describing the interacting plasma as a system of massive quasiparticles (QPs); section 2 gives a short review of this technique. While in their simple QP model the (thermal) masses of the quarks and gluons are approximated by the asymptotic limit of the hard-thermal-loop (HTL) self-energies, we consider models based on the HTL-resummed entropy [9, 10, 11], which include more of the physically important plasmon effect than in the simple QP model, and (NLO) extensions thereof, which include the full plasmon effect. In perturbation theory it is essentially this effect that spoils convergence, so a priori it was not granted that a model including this effect fully would give physically sensible results. As it turns out, however, the results based on our models (which are presented in section 3 and 4, respectively) turn out to be well-behaved and indeed lie not too far from the simple QP model.

In section 5 we give the 2-parameter fits of the various models to the lattice data [27] for 2 flavors and compare the model results for the pressure at small temperatures and large chemical potential in section 6. Furthermore, we compare our results for the isobar emerging at² T_c to recent lattice results and give our conclusions in section 7.

II. MAPPING LATTICE DATA TO FINITE CHEMICAL POTENTIAL USING QP MODELS

Assuming an $SU(N)$ plasma of gluons and N_f light quarks in thermodynamic equilibrium can be described as a weakly interacting gas of massive quasiparticles with residual interaction B , the pressure of the system is given by [23]

$$P(T, \mu) = \sum_{i=g,q} p_i(T, \mu_i, m_i^2) - B(m_g, m_q), \quad (1)$$

where the sum runs over gluons (g), quarks and anti-quarks (q) with respective chemical potential $0, \pm\mu$; p_i are the model dependent QP pressures and m_i are the QP masses. The latter are functions of an effective strong coupling $G^2(T, \mu)$, which appears only within $m_i(G^2, T, \mu)$ in a predefined form.

Using the stationarity of the thermodynamic potential under variation of the self-energies and Maxwell's relations [23], one obtains a partial differential equation for G^2 ,

$$a_T \frac{\partial G^2}{\partial T} + a_\mu \frac{\partial G^2}{\partial \mu} = b, \quad (2)$$

where a_T , a_μ and b are coefficients that are given by integrals depending on T, μ and G^2 . Given a valid boundary condition, a solution for $G^2(T, \mu)$ is found by solving the above flow equation by the method of characteristics; once G^2 is thus known in the T, μ plane, the QP pressure is fixed completely. The residual interaction B is then given by the integral

$$B = \int \sum_i \frac{\partial p_i}{\partial m_i^2} \left(\frac{\partial m_i^2}{\partial \mu} d\mu + \frac{\partial m_i^2}{\partial T} dT \right) + B_0, \quad (3)$$

where B_0 is an integration constant that has to be fixed by lattice data (usually by requiring $P(T_c, \mu = 0) = P_{lattice}(T_c)$). Motivated by the fact that at $\mu = 0$ and $T \gg T_c$ the coupling should

² Here and in the following T_c is always to be understood as $T_c|_{\mu=0}$.

behave as predicted by the perturbative QCD beta-function, Ref. [23] used the ansatz

$$G^2(T, 0) = \frac{48\pi^2}{(11N - 2N_f) \ln \frac{T+T_s}{T_c} \lambda}. \quad (4)$$

The parameters λ and T_s are determined by fitting the entropy of the model (which is independent of B) to available lattice data at $\mu = 0$. Using (4) as boundary condition for (2), the above procedure allows one to map the lattice pressure from $\mu = 0$ to the whole T, μ -plane.

III. SIMPLE AND HTL QP MODEL

A simple ansatz for the QP pressure is obtained by taking p_i to be the pressure of a free gas of massive particles [23, 24], with the masses defined as the asymptotic (i.e. large momentum) gluonic and fermionic self-energies, respectively [28]:

$$\hat{m}_\infty^2 = (2N + N_f) \frac{G^2 T^2}{12} + N_f \frac{G^2 \mu^2}{4\pi^2}, \quad (5)$$

$$\hat{M}_\infty^2 = \frac{G^2(N^2 - 1)}{8N} \left(T^2 + \frac{\mu^2}{\pi^2} \right). \quad (6)$$

Comparing with perturbation theory one finds that while the Stefan-Boltzmann and leading-order interaction terms are correctly reproduced, only $1/(4\sqrt{2})$ of the NLO term of the interaction pressure (the plasmon effect $\sim G^3 T^4$) is present [10].

To include more of this physically relevant effect, one can make use of the HTL-resummed entropy [9, 10, 11], which takes into account the momentum dependence of the QP excitations as well as Landau-damping effects. The HTL model ansatz for the QP pressure for gluons (p_g) and quarks p_q then reads

$$p_g = -d_g \int \frac{d^3 k}{(2\pi)^3} \int_0^\infty \frac{d\omega}{2\pi} n(\omega) \left[2\text{Im} \ln \left(-\omega^2 + k^2 + \hat{\Pi}_T \right) - 2\text{Im} \hat{\Pi}_T \text{Re} \hat{D}_T \right. \\ \left. + \text{Im} \ln \left(k^2 + \hat{\Pi}_L \right) + \text{Im} \hat{\Pi}_L \text{Re} \hat{D}_L \right] \quad (7)$$

$$p_q = -d_q \int \frac{d^3 k}{(2\pi)^3} \int_0^\infty \frac{d\omega}{2\pi} (f_+(\omega) + f_-(\omega)) \left[\text{Im} \ln \left(k - \omega + \hat{\Sigma}_+ \right) \right. \\ \left. - \text{Im} \hat{\Sigma}_+ \text{Re} \hat{\Delta}_+ + \text{Im} \ln \left(k + \omega + \hat{\Sigma}_- \right) + \text{Im} \hat{\Sigma}_- \text{Re} \hat{\Delta}_- \right], \quad (8)$$

where $d_g = 2(N^2 - 1)$, $d_q = 2NN_f$ for gluons and quarks/anti-quarks, respectively; $n(\omega)$ and $f_\pm(\omega)$ are the bosonic and fermionic distribution functions. $\hat{D}_{T,L}$, $\hat{\Delta}_\pm$ are the HTL propagators with $\hat{\Pi}_{T,L}$ and $\hat{\Sigma}_\pm$ the corresponding self-energies,

$$\hat{\Pi}_L(\omega, k) = \hat{m}_D^2 \left[1 - \frac{\omega}{2k} \ln \frac{\omega + k}{\omega - k} \right] \quad (9)$$

$$\hat{\Pi}_T(\omega, k) = \frac{1}{2} \left[\hat{m}_D^2 + \frac{\omega^2 - k^2}{k^2} \hat{\Pi}_L \right] \quad (10)$$

$$\hat{\Sigma}_\pm = \frac{\hat{M}^2}{k} \left[1 - \frac{\omega \mp k}{2k} \ln \frac{\omega + k}{\omega - k} \right]; \quad (11)$$

which we have written in terms of the HTL Debye mass squared $\hat{m}_D^2 = 2\hat{m}_\infty^2$ and the HTL zero-momentum quark mass squared $\hat{M}^2 = \hat{M}_\infty^2/2$.

The HTL QP model includes 1/4 of the full plasmon effect at $\mu = 0$, which is a factor of $\sqrt{2}$ more than in the simple QP model which only uses the asymptotic HTL masses. The remainder of the plasmon effect is in fact entirely due to NLO corrections to these asymptotic masses at order $G^3 T^2$ [9, 10, 11].

IV. NLO MODELS

The complete (momentum-dependent) NLO corrections to the asymptotic masses of quarks and gluons have not been calculated yet, but as far as the plasmon effect is concerned, these corrections contribute in the averaged form [9, 10]

$$\bar{\delta}m_\infty^2 = \frac{\int dk k n'(k) \text{Re} \delta\Pi_T(\omega = k)}{\int dk k n'(k)} = -\frac{1}{2\pi} G^2 N T \hat{m}_D \quad (12)$$

and similarly

$$\bar{\delta}M_\infty^2 = \frac{\int dk k (f'_+(k) + f'_-(k)) \text{Re} 2k\delta\Sigma_+(\omega = k)}{\int dk k (f'_+(k) + f'_-(k))} = -\frac{(N^2 - 1)/(2N)}{2\pi} G^2 T \hat{m}_D. \quad (13)$$

For the values of the coupling G considered here, these corrections are so large that they give tachyonic masses when treated strictly perturbatively. In Ref. [10] it has been proposed to incorporate these corrections through a quadratic gap equation which works well as an approximation in the exactly solvable scalar $O(N \rightarrow \infty)$ -model, where strict perturbation theory would lead to identical difficulties. However, for the fermionic asymptotic masses, in order to have the correct scaling of Casimir factors in the exactly solvable large- N_f limit of QCD [29], a corresponding gap equation has to remain linear in the fermionic mass squared. Choosing the correction therein to be determined by the solution to the gluonic gap leads to [11, 30]

$$\bar{m}_\infty^2 = \hat{m}_\infty^2 - \frac{G^2 N T}{\sqrt{2\pi}} \bar{m}_\infty \quad (14)$$

$$\bar{M}_\infty^2 = \hat{M}_\infty^2 - \frac{G^2 (N^2 - 1) T}{2\sqrt{2\pi} N} \bar{m}_\infty, \quad (15)$$

where \hat{m}_∞^2 and \hat{M}_∞^2 are the leading-order gluonic and fermionic asymptotic masses as given in (5) and (6). This in fact avoids tachyonic masses for the fermions as long as $N_f \leq 3$.³

Finally, since the averaged quantities \bar{m}_∞^2 and \bar{M}_∞^2 are the effective masses at hard momenta only, a cutoff scale $\Lambda = \sqrt{2\pi T \hat{m}_D c_\Lambda}$ is introduced that separates soft from hard momenta. The QP pressure for this model, which in the following will be referred to as NLA-model, then separates into a soft and a hard component for both gluons and fermions. The soft parts are given by expressions like (7) and (8), but with Λ as upper limit for the momentum integration. For the hard parts, the momentum integrations run from Λ to ∞ and the mass pre-factors in the HTL self-energies (9,10,11) are replaced by their asymptotic counterparts, $\hat{m}_D^2 \rightarrow 2\bar{m}_\infty^2$ and $\hat{M}^2 \rightarrow \frac{1}{2}\bar{M}_\infty^2$.

The single free parameter c_Λ in Λ can be varied around 1 to obtain an idea of the ‘‘theoretical error’’ of the model. In the following we will consider the range $c_\Lambda = \frac{1}{4}$ to $c_\Lambda = 4$; note that $c_\Lambda = \infty$ corresponds to the HTL-model (which has been used as cross-check) since all hard corrections are

³ For $N_f = 3$ the solutions to the above approximate gap equations happen to coincide with those obtained in the original version of two independent quadratic gap equations of Ref. [10]. For the case $N_f = 2$ considered in this paper, the differences are fairly small. For $N_f > 3$, however, the necessity to avoid tachyonic masses would restrict the range of permissible coupling strength G .

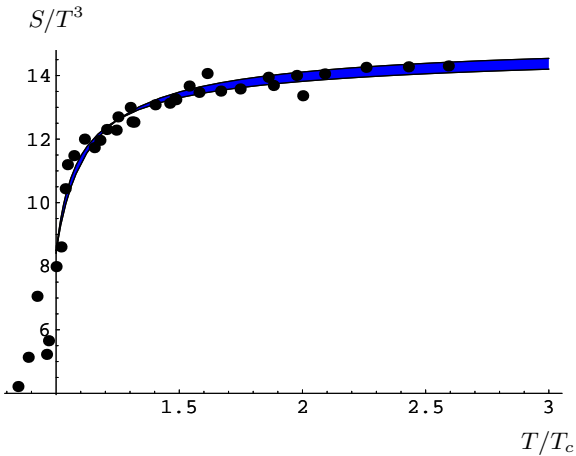


FIG. 1: Entropy data generated from Ref. [27] vs. fitted model entropy. The band was generated from NLA model for c_Λ between 4 and 1; the HTL and simple QP models lie at the lower boundary.

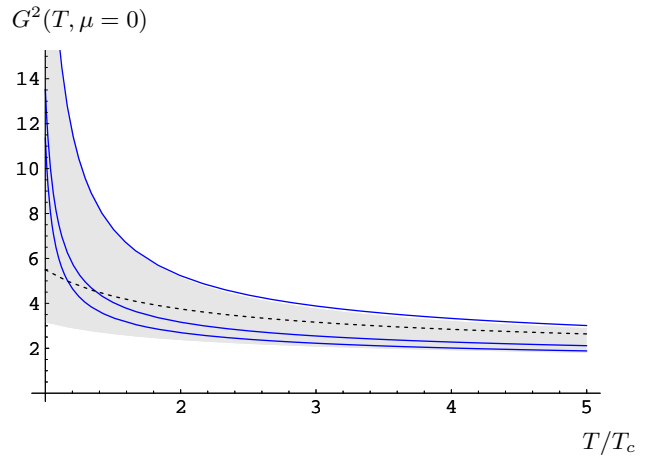


FIG. 2: Effective coupling: NLA model results for $c_\Lambda = 4, 1$ and $1/4$ (full lines from bottom to top), 2-loop perturbative coupling in $\overline{\text{MS}}$ (gray band) and result from Ref.[34] (dotted line).

ignored. On the other hand, $c_\Lambda = 0$ would assume that (14) and (15) represent good approximations for the NLO corrections to the spectral properties of soft excitations. However, the few existing results, in particular on NLO corrections to the Debye mass [31] and the plasma frequency [32], appear to be rather different so that it seems safer to leave the soft sector unchanged by keeping a finite c_Λ .

V. ENTROPY AND PRESSURE FOR $\mu = 0$

To obtain the input parameters T_s and λ we fitted the entropy expressions from the models under consideration to lattice data [27] for $N_f = 2$, with an estimated continuum extrapolation as used in Ref. [24]. We find

	HTL	$c_\Lambda = 4$	$c_\Lambda = 1$	$c_\Lambda = 1/4$
T_s/T_c	-0.89	-0.89	-0.84	-0.61
λ	19.4	18.64	11.43	3.43

where it can be seen that the NLA model with $c_\Lambda = 4$ is very close to the HTL model. The fits to the entropy data (shown in Fig. 1) all lie in a narrow band for all the models considered. The fitted effective coupling G^2 for the various models is shown in figure 2; for comparison, also the 2-loop perturbative running coupling in $\overline{\text{MS}}$ is shown, where the renormalization scale is varied between πT and $4\pi T$ and following Ref. [33] we have chosen $T_c = 0.49\Lambda_{\overline{\text{MS}}}$. As can be seen from the plot, the results for the effective coupling are well within the range of the 2-loop perturbative running coupling (for the case $c_\Lambda = 1/4$ and renormalization scale πT the results even seem to be identical, which is, however, probably only a coincidence). We also show the result for the coupling obtained in the semiclassical approach of Ref. [34]⁴.

In general one can see that the effective coupling becomes bigger when c_Λ gets smaller; this is because the hard masses (for equal values of the coupling) are smaller than the soft masses which

⁴ For finite μ and constant temperatures, however, the coupling obtained in [34] rises while our results indicate a decrease of the coupling (which is consistent with the standard QCD running coupling with renormalization scale proportional to $\sqrt{T^2 + (\mu/\pi)^2}$).

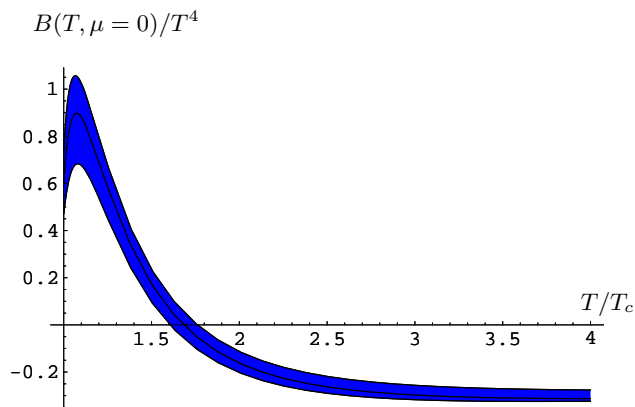


FIG. 3: Residual interaction B : NLA model results between $c_\Lambda = 4$, $c_\Lambda = 1$ (full line) and $c_\Lambda = 1/4$ (lower boundary).

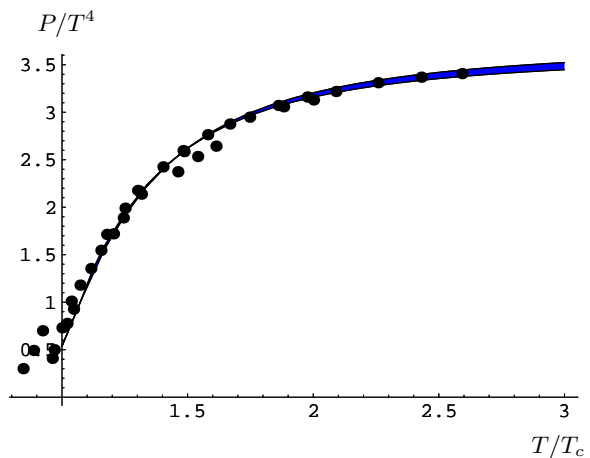


FIG. 4: Pressure data from Ref.[27] vs. model pressure. The band shows the NLA model results for c_Λ between 4 and 1/4.

makes the entropy increase when the hard parts become more important. Accordingly, the coupling has to rise in order for the entropy to match the data (therefore, for the extreme case $c_\Lambda = 0$ one finds huge values of the effective coupling constant).

Once the effective coupling is known for $\mu = 0$ one can proceed to evaluate the QP pressure $\sum p_i$ and the residual interaction B from Eq. (3), shown in Fig. 3; in this figure, the HTL results (not shown) would lie marginally above the upper boundary of the band (cf. [35] for a comparison between simple QP and HTL model). A comparison between the full pressure (1) and the lattice data is shown in figure 4, where the integration constant B_0 was set so that $P(T_c) = 0.536(1)$:

	HTL	$c_\Lambda = 4$	$c_\Lambda = 1$	$c_\Lambda = 1/4$
B_0/T_c^4	0.82	0.73	0.6	0.47

VI. FINITE CHEMICAL POTENTIAL

A calculation and subsequent evaluation of the coefficients a_μ , a_T and b in (2) shows that b , in contrast to a_μ and a_T , is strongly model-dependent. Solving the flow equation (2) and integrating B along the characteristics using Eq. (3) one obtains pressure and effective coupling in the whole T, μ plane. Here we focus on the pressure but the calculation of the other thermodynamic quantities is straightforward once the effective coupling and the pressure have been obtained.

Concerning the shape of the characteristics, it has already been noticed in [35] that the crossing of characteristics in the simple QP model [23] does not occur in the HTL-model; this feature is preserved in the NLA models.

A. Lines of constant pressure

It is straightforward to extract from our data the line where $P(T, \mu) = P(T_c, 0)$; for $N_f = 2$, the results for the simple and HTL QP model as well as for the NLA models for $c_\Lambda > 1$ are rather close to each other. For NLA models with $c_\Lambda < 1$, however, the slope of the constant pressure line (until $\mu/T_c = 1$) deviates rapidly from the values found for $c_\Lambda > 1$:

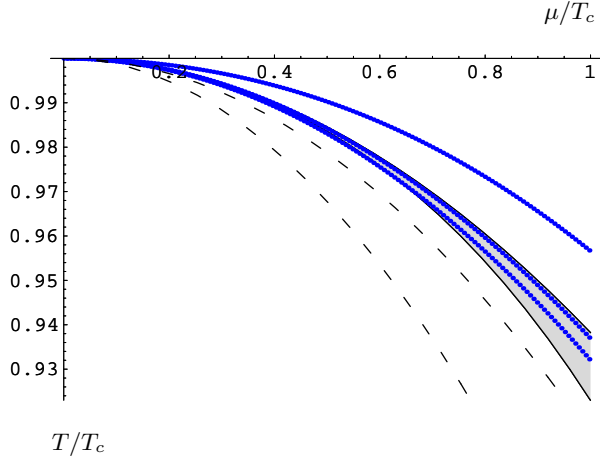


FIG. 5: Lines of constant pressure: NLA models for $N_f = 2$ from $c_\Lambda = 4$, $c_\Lambda = 1$ and $c_\Lambda = 1/4$ (dotted lines from lowest to highest); lattice data for $N_f = 2 + 1$ [20] (light gray band) and $N_f = 2$ [18] (long dashed-lines).

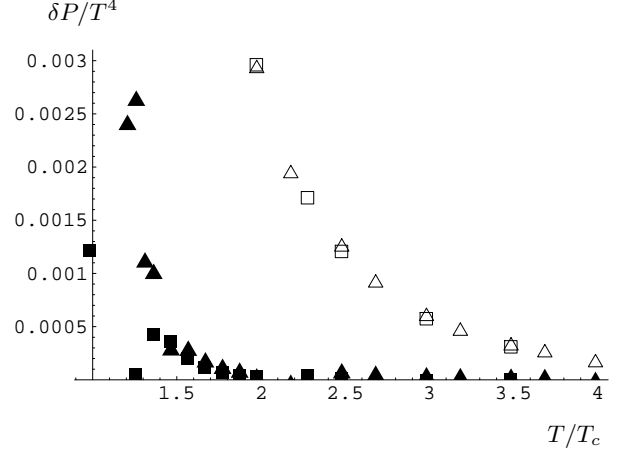


FIG. 6: Difference δP scaled with T^4 for $\mu/T_c = 1$. Shown are HTL model (triangles) and NLA models (boxes). See text for details.

	HTL	$c_\Lambda = 4$	$c_\Lambda = 1$	$c_\Lambda = 1/4$
$T_c \frac{dT}{d\mu^2}$	-0.06818(8)	-0.06810(6)	-0.06329(34)	-0.041(9)

We have also compared these results with recent lattice data for 2+1 flavors [20] in figure 5. The variations of the lattice data in this figure result from fitting the data with a 2nd order (upper limit) and 4th order polynomial (lower limit) as used in [36]. The comparison shows that our 2-flavor results obtained from simple, HTL and NLA QP models with $c_\Lambda > 1$ (indicated in figure 5 by the two lower lying pointed lines) are in very good agreement with the lattice data whereas for NLA models with $c_\Lambda < 1$ the slope is much flatter. Also shown are the lattice results for the constant pressure line from [18] for 2 flavors, with a slope of $T_c \frac{dT}{d\mu^2} = -0.107(22)$, which is significantly steeper.

B. Susceptibilities

It been noticed in [20] that the quantity

$$\frac{\Delta P}{\Delta P_{SB}} = \frac{P(T, \mu) - P(T, 0)}{P_{SB}(T, \mu) - P_{SB}(T, 0)} \quad (16)$$

is essentially μ -independent; we recover a similar scaling behavior for our models. As expected, for small chemical potential this curve is very close to the quark-number susceptibilities $\chi(T)/\chi_0(T)$ obtained at $\mu = 0$. In fact, we found that also for larger μ the pressure can be well approximated by

$$P(T, \mu) - P(T, 0) = \frac{\chi(T)}{2} \left(\mu^2 + \frac{\mu^4}{2\pi^2 T^2} \right). \quad (17)$$

To quantify this assertion we consider the subtracted quantity $\delta P = P(T, \mu) - P(T, 0) - \frac{\chi(T)}{2} \left(\mu^2 + \frac{\mu^4}{2\pi^2 T^2} \right)$, which should be zero, if the pressure at finite chemical potential was fully determined by the susceptibilities at $\mu = 0$ according to (17); the results (scaled with T^4) are shown in figure 6 for $\mu/T_c \simeq 1$. As can be seen, dropping the μ^4 term in Eq. (17) (open symbols) deteriorates the result

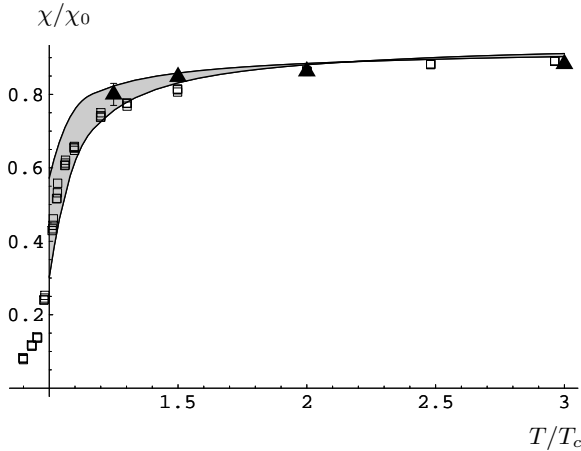


FIG. 7: Susceptibilities from NLA models (light gray band), from $N_f = 2$ lattice data [37] (triangles) and “scaling curve” for 2+1 flavors from [20] (boxes).

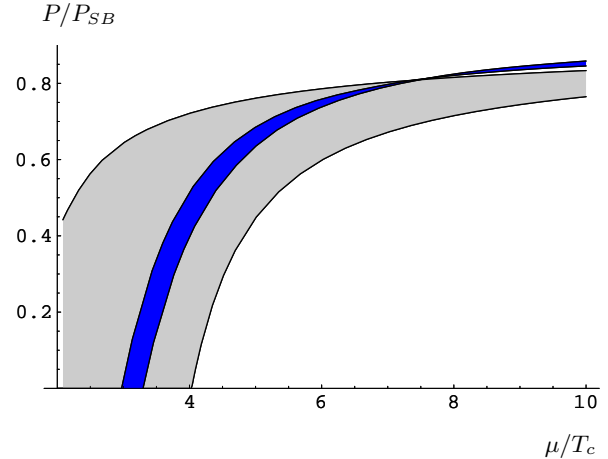


FIG. 8: The pressure at vanishing T : Shown are perturbative results (light gray band) and NLA models for c_Λ from $1/4$ to 4 (dark band).

considerably. Trying to determine the higher-order susceptibility, $\bar{\chi} = \frac{\partial^4 P}{\partial \mu^4}$ which we parameterized as

$$\bar{\chi} = \frac{\chi(T)}{2T^2} \frac{4!}{x(T)^2},$$

we find that – within our numerical errors – the result for $x(T)$ is consistent with $\sqrt{2}\pi = 4.44\dots$ for $T > 1.5T_c$ (which was our original assumption in Eq. (17)); therefore, our results are close to but about 10 percent lower than the values found in Ref. [22].

Clearly, δP gets smaller with increasing temperature, but also at relatively low temperatures and high chemical potential, δP is remarkably small (e.g., for the HTL model for $T = 1.5T_c$ and $\mu/T_c \simeq 4$ we find a $\delta P/T^4$ smaller than 10 percent).

In Fig. 7 we compare the results for the susceptibilities of our NLA models with the lattice data for 2 flavors from Ref. [37] and the “scaling curve” in [20], which provides an approximation to the 2+1 flavor quark-number susceptibility at $\mu = 0$. We find that all these results agree very well, with the agreement getting better at higher temperatures.

It should be noted however that none of the lattice data we are using has yet been rigorously extrapolated to the continuum limit, so that both the data and the extrapolation by means of QP models are still likely to change somewhat when this will be done eventually.

C. Very small temperatures

Extending the lines of constant pressure from our models to very small temperatures we obtain a crude estimate of the phase transition line in this region of phase space. Denoting with μ_c the chemical potential where (for vanishing temperature) the pressure equals the lattice pressure at $\mu = 0$, $P(0, \mu_c) = P(T_c, 0)$, we find for our models (assuming $T_c = 172$ MeV)

	HTL	$c_\Lambda = 4$	$c_\Lambda = 1$	$c_\Lambda = 1/4$
μ_c	533 MeV	536 MeV	558 MeV	584 MeV
μ_0	509 MeV	511 MeV	537 MeV	567 MeV

Here we have also given the values μ_0 where the pressure vanishes, which may be taken as a definite lower bound for the critical chemical potential within the respective models.

In general, these results are in agreement with the estimates for μ_c from [24, 36]; for the QP models considered, the lowest and highest results for μ_c are obtained for the HTL model and the NLA model with $c_\Lambda = 1/4$, respectively, while the μ_c of the simple QP model lies between the NLA $c_\Lambda = 4$ and $c_\Lambda = 1$ model values. However, even our lowest result for μ_c turns out to exceed the value for the critical chemical potential expected in Ref. [25, 38].

A comparison of the perturbative pressure [39] at vanishing temperature with the results for our models at $T/T_c \simeq 0.01$ is shown in figure 8. We plotted the perturbative results converted to $\overline{\text{MS}}$ with the standard 2-loop running coupling, $\Lambda_{\overline{\text{MS}}} = T_c/0.49$ [33] and renormalization scale varied from μ to 3μ ; a comparison of this coupling and our results is shown in figure 9.

D. Equation of state for cold dense matter

By calculating the number density at $T/T_c \simeq 0.01$ and using our results for the pressure we obtain an equation of state for cold deconfined matter. As is the case for the simple QP model [24], we find that the energy density \mathcal{E} is well fitted by the linear relation

$$\mathcal{E}(p) = 4\tilde{B} + \alpha p$$

with

	HTL	$c_\Lambda = 4$	$c_\Lambda = 1$	$c_\Lambda = 1/4$
$4\tilde{B}/T_c^4$	11.1(8)	12.3(8)	14.7(9)	19.2(1.6)
α	3.23(5)	3.22(4)	3.22(4)	3.17(4)

A value of $\alpha \simeq 3.2$ for $N_f = 2$ has also been found in the simple quasiparticle model in [24] and thus seems to be model independent, in contrast to the bag constant $\tilde{B}^{1/4}$, which varies between 314 and 360 MeV. By using the Tolman-Oppenheimer-Volkov equations and the equation of state one can determine the mass-radius relations of non-rotating quark-stars [26]; choosing $\alpha = 3.2$ and taking the bag constant values from above, we find stable star configurations with radii ranging from 3.6 to 4.9 km and masses from 0.7-0.8 solar masses for NLA, $c_\Lambda = 1/4$ and HTL models, respectively. However, it should be kept in mind that the outermost layers of such a quark star are metastable with respect to hadronic matter and therefore the details of the star structure will depend sensitively on the hadronic equation of state [24].

VII. CONCLUSIONS AND OUTLOOK

We considered an improvement of simple quasiparticle models [23] by using the full HTL approximation and certain NLO corrections thereof along the lines of Ref. [9, 10, 11] and investigated the respective predictions at finite chemical potential when these models are matched to $N_f = 2$ lattice data at $\mu = 0$.

We found that the slope of constant pressure for those models with $c_\Lambda > 1$ agrees very well with recent lattice data for 2+1 flavors [20, 36], while the lattice data for $N_f = 2$ [18] indicate significantly steeper slopes.

We also found that for our models the pressure for non-vanishing μ scales with the quark number susceptibilities at $\mu = 0$, provided that the μ^4 terms (corresponding to a higher order susceptibility) are not dropped but added with the same weight as in the ideal gas limit. We therefore interpreted the “scaling curve” from 2+1 flavor lattice data [20] as susceptibilities at $\mu = 0$ and found that a comparison with $N_f = 2$ susceptibilities from another lattice group [37] as well as those obtained from our models all agree very well.

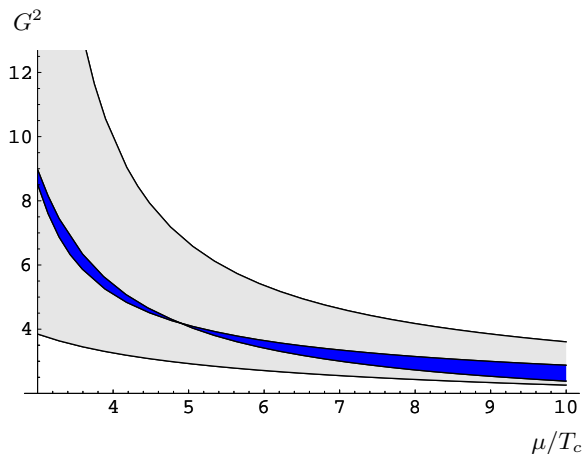


FIG. 9: Effective Coupling from NLA models with $c_\Lambda = 4$ to $1/4$ (dark band) and perturbative 2-loop running coupling (light gray band).

We finally extended our results to the small temperature, high density regime and obtained an estimate for the critical density at $T = 0$ which is consistent with earlier results, though in excess of the expectations of Ref. [25, 38]. Furthermore, we obtained an equation of state for cold, dense matter, which allows for pure quarks stars with masses of $\sim 0.8M_\odot$ and radii of less than 5 km, similar to the results obtained by [24, 25, 40].

Acknowledgments

We want to thank Z. Fodor and K.K. Szabo for kindly providing their lattice data and A. Peshier, C. Schmidt and R.A. Schneider for discussions. This work has been supported by the Austrian Science Foundation FWF, project no. 14632.

-
- [1] J. C. Collins and M. J. Perry, Phys. Rev. Lett. **34**, 1353 (1975).
 - [2] M. Alford, Lect. Notes Phys. **583**, 81 (2002) and references therein.
 - [3] P. Arnold and C.-X. Zhai, Phys. Rev. **D51**, 1906 (1995).
 - [4] C.-X. Zhai and B. Kastening, Phys. Rev. **D52**, 7232 (1995).
 - [5] K. Kajantie, M. Laine, K. Rummukainen, and Y. Schröder, The pressure of hot QCD up to $g^6 \ln(1/g)$, hep-ph/0211321.
 - [6] E. Braaten and R. D. Pisarski, Phys. Rev. **D45**, 1827 (1992); J. Frenkel and J. C. Taylor, Nucl. Phys. **B374**, 156 (1992); J. P. Blaizot and E. Iancu, Nucl. Phys. **B417**, 608 (1994).
 - [7] J. O. Andersen, E. Braaten, and M. Strickland, Phys. Rev. Lett. **83**, 2139 (1999); Phys. Rev. **D61**, 014017, 074016 (2000).
 - [8] J. O. Andersen, E. Braaten, E. Petitgirard, and M. Strickland, Phys. Rev. **D66**, 085016 (2002); J. O. Andersen, E. Petitgirard, and M. Strickland, Two-loop HTL Thermodynamics with Quarks, hep-ph/0302069.
 - [9] J. P. Blaizot, E. Iancu, and A. Rebhan, Phys. Rev. Lett. **83**, 2906 (1999); Phys. Lett. **B470**, 181 (1999).
 - [10] J. P. Blaizot, E. Iancu, and A. Rebhan, Phys. Rev. **D63**, 065003 (2001).
 - [11] J.-P. Blaizot, E. Iancu, and A. Rebhan, Thermodynamics of the high-temperature quark gluon plasma, hep-ph/0303185.
 - [12] A. Peshier, Phys. Rev. **D63**, 105004 (2001).
 - [13] J. P. Blaizot, E. Iancu, and A. Rebhan, On the apparent convergence of perturbative QCD at high temperature, hep-ph/0303045.

- [14] E. Braaten and A. Nieto, Phys. Rev. **D53**, 3421 (1996).
- [15] F. Karsch, Lect. Notes Phys. **583**, 209 (2002).
- [16] E. Laermann and O. Philipsen, The Status of Lattice QCD at Finite Temperature, hep-ph/0303042.
- [17] Z. Fodor and S. D. Katz, Phys. Lett. **B534**, 87 (2002); JHEP **0203**, 014 (2002).
- [18] C. R. Allton *et al.*, Phys. Rev. **D66**, 074507 (2002); The equation of state for two flavor QCD at non-zero chemical potential, hep-lat/0305007.
- [19] P. de Forcrand and O. Philipsen, Nucl. Phys. **B642**, 290 (2002).
- [20] Z. Fodor, S. D. Katz, and K. K. Szabo, The QCD equation of state at nonzero densities: Lattice result, hep-lat/0208078, 2002.
- [21] M. D'Elia and M.-P. Lombardo, Phys. Rev. **D67**, 014505 (2003).
- [22] R. V. Gavai and S. Gupta, Pressure and non-linear susceptibilities in QCD at finite chemical potentials, hep-lat/0303013, 2003.
- [23] A. Peshier, B. Kämpfer, and G. Soff, Phys. Rev. **C61**, 045203 (2000).
- [24] A. Peshier, B. Kämpfer, and G. Soff, Phys. Rev. **D66**, 094003 (2002).
- [25] E. S. Fraga, R. D. Pisarski, and J. Schaffner-Bielich, Nucl. Phys. **A702**, 217 (2002).
- [26] J. O. Andersen and M. Strickland, Phys. Rev. **D66**, 105001 (2002).
- [27] A. Ali Khan *et al.*, Phys. Rev. **D64**, 074510 (2001).
- [28] F. Flechsig and A. K. Rebhan, Nucl. Phys. **B464**, 279 (1996).
- [29] G. D. Moore, JHEP **0210**, 055 (2002); A. Ipp, G. D. Moore, and A. Rebhan, JHEP **0301**, 037 (2003).
- [30] A. Rebhan, HTL-resummed thermodynamics of hot and dense QCD: An update, hep-ph/0301130.
- [31] A. K. Rebhan, Phys. Rev. **D48**, 3967 (1993); Nucl. Phys. **B430**, 319 (1994).
- [32] H. Schulz, Nucl. Phys. **B413**, 353 (1994).
- [33] S. Gupta, Phys. Rev. **D64**, 034507 (2001).
- [34] R. A. Schneider, The QCD running coupling at finite temperature and density, hep-ph/0303104.
- [35] P. Romatschke, Cold deconfined matter EOS through an HTL quasi-particle model, hep-ph/0210331.
- [36] K. K. Szabo and A. I. Toth, Quasiparticle Description of the QCD Plasma, Comparison with Lattice Results at Finite T and μ , hep-ph/0302255.
- [37] R. V. Gavai, S. Gupta, and P. Majumdar, Phys. Rev. **D65**, 054506 (2002).
- [38] E. S. Fraga, R. D. Pisarski, and J. Schaffner-Bielich, Phys. Rev. **D63**, 121702 (2001).
- [39] B. A. Freedman and L. D. McLerran, Phys. Rev. **D16**, 1169 (1977).
- [40] D. Blaschke *et al.*, Phys. Lett. **B450**, 207 (1999).